hydrogen

MDPI

Article

Sustainable Hydrogen Production from Plastic Waste: Optimizing Pyrolysis for a Circular Economy

Fiyinfoluwa Joan Medaiyese *, Hamid Reza Nasriani, Khalid Khan and Leila Khajenoori

School of Engineering & Computing, University of Central Lancashire, Preston PR1 2HE, UK; hrnasriani@uclan.ac.uk (H.R.N.); kkhan5@uclan.ac.uk (K.K.); lkhajenoori@uclan.ac.uk (L.K.)
* Correspondence: fjmedaiyese@uclan.ac.uk

Abstract: Hydrogen is a clean, non-polluting fuel and a key player in decarbonizing the energy sector. Interest in hydrogen production has grown due to climate change concerns and the need for sustainable alternatives. Despite advancements in waste-to-hydrogen technologies, the efficient conversion of mixed plastic waste via an integrated thermochemical process remains insufficiently explored. This study introduces a novel multi-stage pyrolysis-reforming framework to maximize hydrogen yield from mixed plastic waste, including polyethylene (HDPE), polypropylene (PP), and polystyrene (PS). Hydrogen yield optimization is achieved through the integration of two water–gas shift reactors and a pressure swing adsorption unit, enabling hydrogen production rates of up to 31.85 kmol/h (64.21 kg/h) from 300 kg/h of mixed plastic wastes, consisting of 100 kg/h each of HDPE, PP, and PS. Key process parameters were evaluated, revealing that increasing reforming temperature from 500 °C to 1000 °C boosts hydrogen yield by 83.53%, although gains beyond 700 °C are minimal. Higher reforming pressures reduce hydrogen and carbon monoxide yields, while a steam-to-plastic ratio of two enhances production efficiency. This work highlights a novel, scalable, and thermochemically efficient strategy for valorizing mixed plastic waste into hydrogen, contributing to circular economy goals and sustainable energy transition.

Keywords: hydrogen; pyrolysis; pyrolysis and in-line reforming; steam reforming; plastic wastes; waste plastics; Aspen Plus; simulation; optimization

Academic Editor: Isabel Cabrita

Received: 30 January 2025
Revised: 27 February 2025
Accepted: 1 March 2025
Published: 7 March 2025

Citation: Medaiyese, F.J.; Nasriani, H.R.; Khan, K.; Khajenoori, L. Sustainable Hydrogen Production from Plastic Waste: Optimizing Pyrolysis for a Circular Economy. *Hydrogen* **2025**, *6*, 15. https://doi.org/10.3390/hydrogen6010015

1. Introduction

The increasing demand for energy, concerns over climate change, and the depletion of fossil fuel resources have driven extensive research into the exploration of alternative and eco-friendly energy sources such as hydrogen [1]. Global energy demand is increasing substantially due to factors such as economic development, rising living standards, and population growth [2,3]. This trend is anticipated to persist in the coming decades, posing notable implications for energy production, consumption, and policy. The global population is projected to reach 9.7 billion by 2050, adding 1.7 billion new energy consumers. This population growth, along with economic development, is a key factor driving the rise in energy demand [4]. The growing energy demand is closely linked to rising greenhouse gas emissions, presenting a major obstacle to achieving global climate objectives. To limit the increase in global temperatures to below 2 °C, as outlined in the Paris Climate Agreement, considerable efforts in energy efficiency and the widespread adoption of low-carbon technologies are necessitated [3]. Therefore, harnessing sustainable and renewable energy is necessary to ensure future energy sustainability and global energy security [5].

According to Rohland et al. [6], renewable resources are predicted to have shares of 36% of global energy demand by 2025 and 69% by 2050, while hydrogen will make up 11% in 2025 and 34% in 2050 [7].

Hydrogen is increasingly gaining recognition as a clean and sustainable fuel with the potential to address global energy demands and environmental challenges. This growing interest in hydrogen is reflected in Figure 1, which illustrates the rise in global hydrogen production capacity. Unlike fossil fuels, the combustion of hydrogen only produces water vapor [8], making it a zero-emission fuel capable of reducing air pollution and greenhouse gas emissions. It can be used in transportation, energy storage, power generation, and distributed heating systems [9]. Utilizing hydrogen as a fuel in internal combustion engines reduces emissions of CO, unburned hydrocarbons (UHC), CO_2, and soot, making it a clean and sustainable energy alternative [10,11]. Some sources for hydrogen production include water, glycerol, fossil fuels, and renewable energy sources [9]. Presently, the major source of hydrogen is fossil fuels (naphtha, coal or natural gas) [12–16]. To ensure the sustainability of hydrogen production, alternative sources like renewable biomass and plastics are being investigated [1].

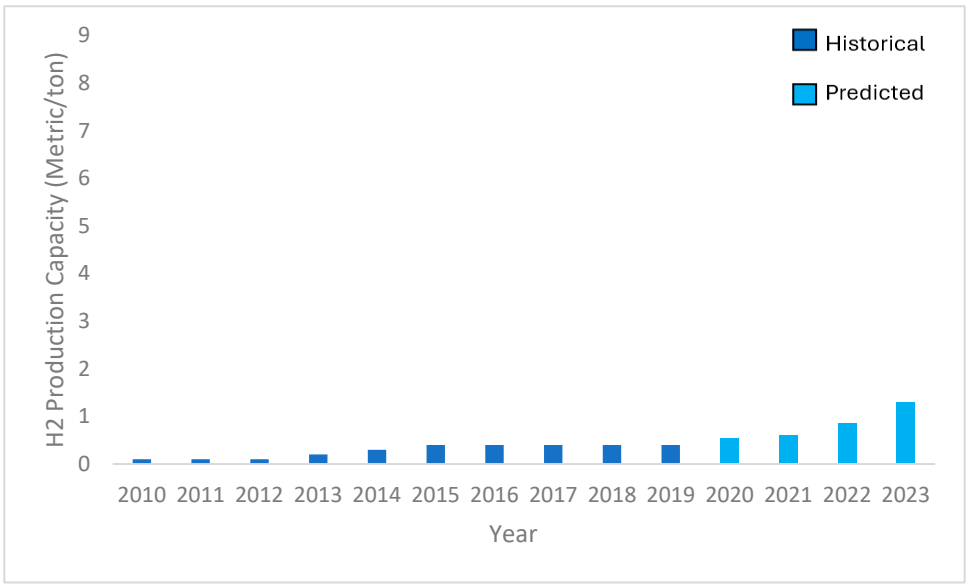

Figure 1. Hydrogen production capacity worldwide in metric tons per year IEA (2010–2023) [9].

Currently, research on hydrogen production from mixed plastic wastes is limited. Consequently, investigating hydrogen production from commonly discarded plastics, such as packaging plastic types, can contribute to sustainable waste management, and analyzing the influence of key parameters can help optimize the process. In this study, the focus is on producing hydrogen from a blend of plastic waste consisting of high-density polyethylene, polypropylene, and polystyrene, with an emphasis on identifying the optimal operating conditions.

Despite increasing research into hydrogen production from waste plastics, most studies concentrate on single-polymer feedstocks or gasification-based processes, leaving multi-polymer pyrolysis with in-line steam reforming largely unexplored. Additionally, few studies provide a detailed thermodynamic equilibrium-based optimization of key process parameters such as temperature, pressure, and steam-to-plastic ratio (S/P ratio). This study introduces a novel multi-stage pyrolysis-reforming framework that integrates slow pyrolysis, in-line steam reforming, water–gas shift reactions, and pressure swing adsorption (PSA) to maximize hydrogen yield from mixed plastic waste. The research provides quantitative insights into the impact of S/P ratio, temperature, and pressure, achieving

a hydrogen yield of 31.85 kmol/h (64.21 kg/h) at optimal conditions, representing an 83.53% increase compared to unoptimized conditions. The findings bridge the gap between theoretical modeling and industrial applicability, offering a scalable, sustainable pathway for transforming plastic waste into clean hydrogen.

Plastic Waste as a Hydrogen Source

Recently, plastic waste as a hydrogen source has been gaining significant attention as a promising "waste-to-value" strategy. This approach aligns with the principles of circular economy by addressing two critical challenges: advancing clean energy solutions and managing plastic waste. With an estimated 8.3 billion tons of non-biodegradable plastics produced globally, over 75% are discarded as waste; hence, transforming this abundant plastic waste into value-added fuels such as hydrogen aligns with global efforts to achieve carbon neutrality [17].

Plastic packaging constitutes a substantial share of overall plastic waste, driven by the extensive use of plastics in the packaging industry compared to other sectors. In the UK, approximately 5 million tonnes of plastic are consumed annually, with nearly half used for packaging [18]. The major types of packaging plastics include the following: Polyethylene terephthalate (PET), low-density polyethylene (LDPE), high-density polyethylene (HDPE), polypropylene (PP) and polystyrene (PS). Although PET is among the most widely used plastic in modern daily life, its composition, including terephthalic acid and oxygen, makes it less suitable as a feedstock for thermochemical processes like pyrolysis. This is because these components result in the formation of water and other oxygenated compounds, lowering the calorific value of the resulting fuel [19]. Additionally, the presence of oxygen in its polymer structure leads to the formation of CO and CO_2, which reduces the yield of hydrocarbons available for reforming to produce hydrogen [19,20]. This leads to low hydrogen-to-carbon ratios in its syngas yield. In contrast, polyolefinic plastics serve as excellent sources of hydrogen owing to their higher carbon and hydrogen contents [19–21]. The oxygenates and aromatics produced from the decomposition of PET also lead to carbon deposition, which deactivates the reforming catalyst [20,22]. For these reasons, PET is excluded from this study. One approach to generating hydrogen from plastic waste is via a thermochemical process. Hydrogen can be derived from plastics via two primary thermochemical routes, namely, single-stage gasification and pyrolysis combined with in-line reforming [17]. While single-stage gasification primarily produces hydrogen-rich syngas in a single step, pyrolysis combined with in-line reforming generates gaseous hydrocarbons, which can be further processed in an additional stage to produce hydrogen-rich syngas. The pyrolysis and in-line reforming process approach offers some significant advantages over traditional single-step waste plastic gasification. The primary challenge in single-stage plastic gasification, regardless of the gasifying agent used, is the production of tar in the gas product. However, when O_2 or air is used instead of steam, tar yield is significantly lower due to steam gasification operating at lower temperatures compared to O_2 or air gasification [23,24]. For syngas to be viable for energy production in turbines and engines, its tar content must be below 10 mg N/m^3 and even lower for syngas applications [24]. Tar-related issues, particularly its deposition in process equipment such as heat exchangers, are influenced by its dew point [25]. The dew point is influenced by both the tar composition and concentration. Single-ring aromatic hydrocarbons remain non-condensable even at concentrations as high as 10 g/Nm^3. However, polyaromatic compounds with more than four rings begin to condense at concentrations as low as 1 mg/ Nm^3, resulting in severe operational challenges [26]. Therefore, a key advantage of the pyrolysis-reforming process is its ability to achieve complete conversion, resulting in a tar-free gaseous stream with high hydrogen concentration and no liquid hydrocarbons [24]. Consequently, various studies

have reported H_2 yields exceeding 30 wt% [27–32], which is higher than typical values (less than 20 wt%) from single-stage gasification [33–36]. Moreover, this process operates at lower temperatures compared to single-stage gasification, with the flexibility to select different temperatures for the pyrolysis and reforming stages. For instance, Chai et al. [37] conducted a two-stage pyrolysis and reforming process using a mixture of waste plastics and biomass. The pyrolysis stage took place at 500 °C, followed by the reforming stage at 850 °C. They reported that this two-step approach provided better control over reaction conditions, leading to improved hydrogen production in the gaseous product composition. Furthermore, the two-step method prevents direct contact between plastic impurities and the reforming catalyst [21,35,38]. The pyrolysis-reforming process has demonstrated a remarkable ability to produce hydrogen from a variety of biomass, waste plastics, and other feedstocks [21,39–41]. In previous studies conducted by Barbarias et al. [20], the highest hydrogen production was achieved during pyrolysis-reforming of polyolefins, with 37.3 wt% for HDPE and 34.8 wt% for PP. The lower hydrogen content in the composition of PS resulted in a lower H_2 yield of 29.1 wt%. Similarly, when PET was used as a feedstock, the hydrogen production was only 18.2 wt%, roughly half of the yield obtained from HDPE pyrolysis-reforming. This lower yield was attributed to both the composition of PET and the formation of carbonaceous residue during the pyrolysis step. Notably, this process provides a sustainable pathway for hydrogen production from waste materials, in contrast to the current global hydrogen generation, which largely relies on fossil fuels such as oil, coal, and natural gas [21,42–46].

The pyrolysis and in-line reforming process involves (i) pyrolysis of plastic to yield volatile hydrocarbons (ii) in-line reforming of the produced gases to yield syngas comprising hydrogen and carbon monoxide [47]. Pyrolysis is a chemical recycling method involving a chemical reaction that breaks down plastics at moderate to high temperatures (400–600 °C) in the absence of oxygen, resulting in the production of low-molecular-weight compounds such as oil or gas. Unlike other reforming methods such as partial oxidation, auto-thermal reforming, or dry reforming, steam reforming does not require oxygen or CO_2 as a reforming agent but steam. This simplicity, combined with its high thermal efficiency of up to 85%, makes it widely used in industrial applications [48]. On the other hand, dry reforming also offers distinct advantages, particularly its ability to utilize CO_2 and is thermodynamically advantageous owing to its low enthalpy. However, the hydrogen yield in dry reforming is reduced due to the reverse water–gas shift reaction that occurs, which generates additional carbon oxides, thereby lowering the H_2/CO ratio [48,49]. Some authors utilize tri-reforming of methane for hydrogen production, which involves three reforming agents: steam, CO_2, and oxygen. However, this technology remains in its early stages, with many technical challenges yet to be addressed [50].

Steam reforming involves the reaction of hydrocarbons with high-temperature steam (700–1000 °C) under moderate pressure in the presence of a nickel-based catalyst to primarily produce hydrogen and carbon monoxide [47]. The general chemical reaction for the steam reforming reaction is represented in Equation (1).

$$C_nH_m + nH_2O \rightarrow nCO + \left(n + \frac{m}{2}\right)H_2 \quad (1)$$

The syngas produced is further processed to enhance the hydrogen yield through the water gas shift reaction, where the carbon monoxide reacts with steam to form carbon dioxide and hydrogen as depicted in Equation (2).

$$CO + H_2O \leftrightarrow CO_2 + H_2 \quad \Delta H_{298K} = -41 kJ/mol \quad (2)$$

The commercial hydrogen production process typically employs two stages of water–gas shift reactions: a high-temperature water–gas shift reaction (310–450 °C) followed by a low-temperature water–gas shift reaction (200–250 °C). These reactions are usually operated in series and configured as fixed-bed reactors. Afterward, hydrogen is purified from the other gases, typically using a pressure swing adsorption system [47].

The key operating parameters for pyrolysis and in-line reforming of biomass, as identified by Arregi et al. [43], Barbarias et al. [51], and Isicheli et al. [52] include reforming temperature and steam/carbon ratio. Arregi et al. [32] highlighted the significance of the exothermic WGS reaction, noting that it is favorable at low temperatures, with H_2 and CO_2 as the primary products.

2. Methodology

Aspen Plus V14.0 was utilized to design and simulate the pyrolysis and in-line reforming process. This software was selected for modeling and simulating the hydrogen production process due to its extensive database, which is crucial for accurately modeling and simulating complex chemical processes like plastic waste pyrolysis. A block flow schematic of the simulation model is presented in Figure 2.

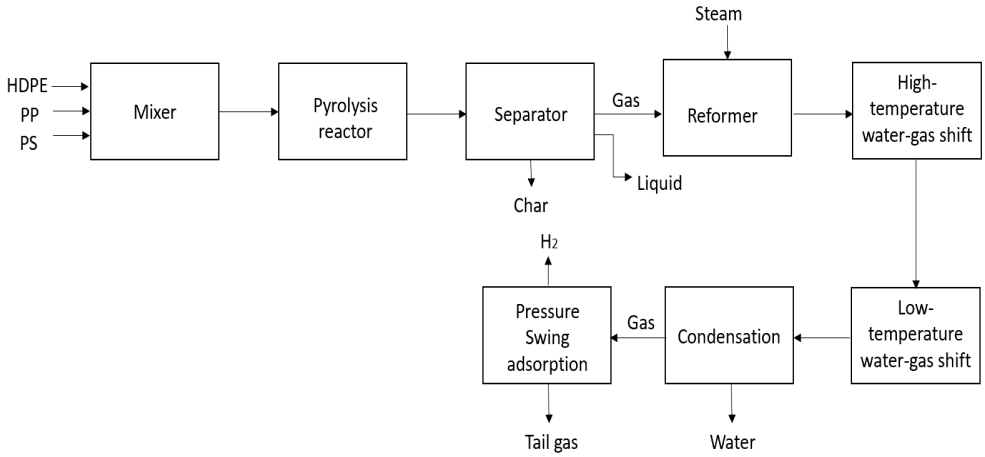

Figure 2. Block flow diagram of pyrolysis and in-line reforming as simulated in Aspen Plus.

As the components needed for the simulation included polymers, the polymer and segments databank (APV 140 Polymer and APV 140 Segment) was incorporated into the enterprise database sheet. The "repeat" type was selected for each segment ID under the polymer tab, while the "pyrolysis" option was chosen for the built-in attribute group of each polymer ID. Table 1 presents the monomers and repeat units/segments associated with each polymer used in the simulation. The repeat unit ID denotes the name assigned to represent the repeat unit within the simulation model.

Table 1. Input required for pyrolysis reaction set.

Polymer	Monomer	Repeat Unit/Segment	Repeat Unit ID
High-density polyethylene (HDPE)	C2H4	Ethylene-R	ETH
Polypropylene (PP)	C3H6	Propylene-R	PP-SEG
Polystyrene (PS)	C8H8	Styrene-R	STY

The other components included in the simulation were based on the GC-MS analysis of products obtained from the individual pyrolysis of the various plastic types used in the simulation, as conducted by various researchers; Sachin et al. for HDPE [53], Sarker et al. for PP [54] and Jaafar et al. [55]. Table 2, Table 3, and Table 4 display the

results of the GC-MS analysis of liquid oil samples obtained from waste HDPE, PP, and PS, respectively.

Table 2. GC-MS analysis of liquid oil sample from waste HDPE [53].

Compound Name	Compound Formula/Component ID
1-Nonene	C9H18
Nonane	C9H20
1-Decene	C10H20
Decane	C10H22
1-Undecene	C11H22
Undecane	C11H24
1-Dodecene	C12H24
Dodecane	C12H26
1-Tridecene	C13H28
Tridecane	C13H28
1-Tetradecene	C14H28
Tetradecane	C14H30
1-Pentadecene	C15H30
Pentadecane	C15H32
Hexadecane	C16H34
1-Heptadecene	C17H34
1-Nonadecene	C19H38
Eicosane	C20H42
Heneicosane	C16H34
Docosane	C22H46
Tricosane	C23H48
Tetracosane	C24H50
N-Tetracosanol-1	C24H50O
4,6-Dimethyldodecane	3:5-D-01

Table 3. GC-MS analysis of liquid oil sample from waste PP [54].

Compound Name	Chemical Formula	Component ID
Pentane	C5H12	N-PEN-01
Cyclopropane,1,2-dimethyl-, cis-	C5H10	1:2-C-01
Pentane, 2-methyl-	C6H12	2-MET-01
1-Pentene, 2-methyl-	C6H14	2-MET-02
2-Pentene, 4-methyl-, (z)	C6H12	4-MET-01
Isopropenylcyclopropane	C6H10	2-CYC-01
1,3-Pentadiene, 2-methyl-,(E)	C6H10	TRANS-01
1-Pentene, 2,4-dimethyl-	C6H10	2:4-D-01
2-Pentene, 3-ethyl-	C7H14	3-ETH-01
2,4-Dimethyl 1,4-pentadiene	C7H12	(E)-2-01
Pentane, 2-bromo-2-methyl-	C6H13BR	PENTA-01
Hexane, 3-methyl-	C7H16	3-MET-01
2-Pentanone	C5H10O	METHY-01
1-Hexene, 2-methyl-	C7H14	2-MET-03
Heptane, 4-methyl-	C8H18	4-MET-02
Cyclohexane, 1,3,5-trimethyl-	C9H18	CIS-1-01
2,4-Dimethyl-1-heptene	C9H18	2:6-D-01
Cyclohexane,1,3,5-	C9H18	1-TRA-01
C10-C13		

Table 4. GC-MS analysis of liquid oil sample from waste PS [55].

Compound Name	Chemical Formula	Component ID
Benzene	C6H6	C6H6
Toluene	C7H8	C7H8
Ethylbenzene	C8H10	C8H10
Styrene	C8H8	STYRENE
Alpha-methylstyrene	C9H10	C9H10
Indene	C9H8	C9H8
Naphthalene	C10H8	C10H8
1,2 Diphenylethane (bibenzyl)	C14H14	C14H14
2,4-Diphenyl-1-butene	C16H16	C16H16
(E)-Stilbene	C14H12	C14H12
1-Phenylnaphthalene	C16H12	C16H12
o-Terphenyl	C18H14	C18H14
2-methylphenanthrene	C15H12	C15H12
2-phenylnaphthalene	C16H12	BETA-01
m-Terphenyl	C18H14	M-TER-01
p-Terphenyl	C18H14	P-TER-01
1,3,5-Triphenylcyclohexane	C27H30	C27H3-01

According to the review conducted by Gebre et al. [56], the gas composition obtained from the pyrolysis of plastic wastes is shown in Table 5.

Table 5. Gas composition from pyrolysis of plastic wastes [56].

Compound Name	Chemical Formula	Component ID
Hydrogen	H2	H2
Methane	CH4	C1
Ethane	C2H6	C2
Ethene/ethylene	C2H4	C2H4
Propane	C3H8	C3
Propene/propylene	C3H6	C3H6
Butane	C4H10	C4
Isobutylene	C4H8	ISOBU-01

The property method, POLYSL (Sanchez–Lacombe), was selected due to its suitability for simulating systems involving polymers, including pyrolysis. The model was designed to simulate the pyrolysis and steam reforming process of three plastics, namely HDPE, PP, and PS, in a ratio of 1:1:1 (100kg/h PE, 100 kg/h PP, and 100 kg/h PS). In the flowsheet, the feed stream comprising the polymer needed to be adequately specified. Certain properties from the attribute list, such as segment mole fractions relative to mole flow of all segments (SFRAC), polydispersity index (PDI), and weight average molecular weight (MWW)/number average molecular weight (MWN), were required. Understanding the weight-average molecular weight (Mw), number-average molecular weight (Mn), and polydispersity index (PDI) of a polymer is essential as they indicate the size of the polymer molecules and the uniformity of their distribution, which are key factors in determining the physical, mechanical and processing properties of the polymer. The component attribute values for each polymer were inputted into Aspen Plus and are presented in Table 6.

The pyrolysis process was modeled with the following assumptions, which were taken into consideration:

- The process operates under steady-state conditions and isothermal;
- The char produced includes only plastic residue;

- The gaseous products comprise light hydrocarbons such as methane, ethane, ethylene, propane, propylene, butane and butylene.

Table 6. Polymer component attribute values.

Polymer	Chemical Formula	MWN	MWW	PDI	SFRAC
HDPE	(C2H4)n	125,000	-	2	1
PP	(C3H6)n	54,000	127,000	-	1
PS	(C8H8)n	98,100	111,800	-	1

Polystyrene (PS), high-density polyethylene (HDPE), and polypropylene (PP), each with a mass flow rate of 100 kg/h at ambient conditions (25 °C, 1 bar), were fed into a mixer to combine into a single mixed plastics stream. This stream was then heated to 500 °C, the pyrolysis temperature. Given that the experimental data utilized for this simulation pertains to slow pyrolysis, a batch reactor was used for modeling the pyrolysis reactor where the pyrolysis reaction took place. The batch reactor operated at 500 °C and 1 bar. The kinetic model chosen for this process was pyrolysis; therefore, three pyrolysis reaction sets were created under the reaction sheet, with the rate constants shown in Tables 7–9. The pyrolysis reaction set in Aspen Plus was selected to automatically generate the main pyrolysis reactions (random-scission, h-abstraction, h-shift, mid-chain beta scission, depolymerization, and termination by disproportion and combination) with the respective monomer and repeat unit according to Table 1 selected for each polymer. These reaction sets were then selected under the kinetics sheet of the batch reactor where the reactions occurred. The thermal conversion of the plastics into products involves activation energies that correspond to the stages of thermal cracking: random scission, hydrogen-abstraction, hydrogen-shift, mid-chain beta scission, depolymerization, and termination by disproportion and termination by combination to form small molecules. The products of the thermal cracking of the plastics can be categorized into hydrogen, rich petroleum gases (C_1-C_4), non-aromatic and aromatic liquids (C_5-C_{12}), waxes (>C_{12}), and char. The products identified from the GC-MS analysis of the pyrolysis of each polymer were inputted into the species sheet for each polymer and categorized according to their respective groups: paraffinic, olefinic, and diolefinic. The rate constants of the pyrolysis of plastics were obtained from experiments conducted by Levine and Broadbelt [57] and Kruse et al. [58,59] for HDPE, PP, and PS, respectively. The pre-exponential and activation energy parameters of the reactions obtained from the experiments were optimized by Aspen Technology [60–62] to fit the input data required in Aspen Plus. The values for each degradation stage are shown in Table 7, Table 8, and Table 9 for HDPE, PP, and PS, respectively.

Table 7. Rate constants for pyrolysis of HDPE [57,60].

Reaction	Pre-Exponential Factor (1/s)	Activation Energy (kcal/mol)
Random scission	9.00×10^{16}	89.7
H-abstraction	2.75×10^{8}	11.2
H-shift	1.00×10^{10}	18.3
Mid-chain beta scission	5.35×10^{14}	28.9
Depolymerization	1.29×10^{12}	28.4
Termination by disproportion	1.10×10^{10}	2.3
Termination by combination	1.10×10^{11}	2.3

Table 8. Rate constants for pyrolysis of PP [58,61].

Reaction	Pre-Exponential Factor (1/s)	Activation Energy (kcal/mol)
Random scission	7.00×10^{16}	82
H-abstraction	1.00×10^{8}	10.5
H-shift	5.00×10^{6}	18.5
Mid-chain beta scission	9.40×10^{14}	28.1
Depolymerization	5.40×10^{13}	28
Termination by disproportion	1.10×10^{10}	2.3
Termination by combination	1.10×10^{11}	2.3

Table 9. Rate constants for pyrolysis of PS [59,62].

Reaction	Pre-Exponential Factor (1/s)	Activation Energy (kcal/mol)
Random scission	5.00×10^{17}	67.3
H-abstraction	2.10×10^{6}	10.5
H-shift	5.00×10^{6}	10.5
Mid-chain beta scission	4.10×10^{12}	28.1
Depolymerization	2.10×10^{12}	24.7
Termination by disproportion	5.50×10^{9}	2.3
Termination by combination	1.10×10^{11}	2.3

The main phases carried out were pyrolysis, steam reforming, water–gas shift reactions, and pressure swing adsorption. The initial stage involved pyrolyzing the plastics to produce the volatile hydrocarbons. The gaseous hydrocarbons, comprising light hydrocarbons including methane, ethane, ethylene, propane, propylene, butane, butylene, and hydrogen, were separated and directed to the reformer. In the reformer, the steam reforming reaction took place, followed by water–gas shift reactions to enhance the hydrogen yield. The steam reformer and water–gas shift reactors were modeled using the Gibbs reactor (RGibbs) module in Aspen Plus. Typically, catalysts are employed in the steam reforming and water–gas shift reaction phases. The catalysts commonly used for steam reforming include rhodium, ruthenium, iron, platinum, and nickel. Although precious metals like rhodium, ruthenium, and platinum have shown superior catalytic activity as a result of their high activation and resistance to carbon deposition, their commercial use is limited by their high cost and limited availability [19,48]. Therefore, cost-effective catalysts like nickel with alumina as catalyst support material (due to its high stability, strength, and surface area) are more commonly used. The high-temperature and low-temperature water–gas shift reactors also utilize different catalysts, with iron-based catalysts for the high-temperature stage and copper-based catalysts for the low-temperature stage [47]. However, for simplicity, this study modeled the reactions using a Gibbs reactor, which assumes reaction equilibrium without relying on kinetic parameters. The Gibbs reactor utilizes Gibbs free energy minimization to calculate the product composition at the equilibrium under well-defined thermodynamic conditions [63]. In the steam reformer, components were transformed into a mixture of carbon monoxide and hydrogen using steam as the reforming agent. In this simulation, water was heated to form steam, which is required as the reforming agent. The reformer was operated at 700 °C and simulated using the restricted chemical equilibrium temperature approach. The following reactions took place in the reformer:

$$CH_4 + H_2O \rightarrow CO + 3H_2 \quad (3)$$

$$C_2H_4 + 2H_2O \rightarrow 2CO + 4H_2 \quad (4)$$

$$C_2H_6 + 2H_2O \rightarrow 2CO + 5H_2 \quad (5)$$

$$C_3H_6 + 3H_2O \rightarrow 3CO + 6H_2 \quad (6)$$

$$C_3H_8 + 3H_2O \rightarrow 3CO + 7H_2 \quad (7)$$

$$C_4H_8 + 4H_2O \rightarrow 4CO + 8H_2 \quad (8)$$

$$C_4H_{10} + 4H_2O \rightarrow 4CO + 9H_2 \quad (9)$$

The property method for the reformer and subsequent unit operations was changed to Peng–Robinson Boston–Mathias (PR-BM) as recommended by Aspen Technology for syngas production. The PR-BM, based on the Peng–Robinson equation of state, is well-suited for syngas production due to its enhanced capability to model both polar and non-polar interactions, robustness across a wide range of conditions, and its accuracy in predicting the behavior of complex gas mixtures. The PR-BM equation of state is particularly effective in high-temperature processes such as reforming [1]. The syngas produced from the reformer was directed into the water–gas shift reactor, where the water–gas shift reaction, as shown in Equation (2), occurred. This reaction was conducted in two separate reactors: the high-temperature water–gas shift (HTWGS) reactor and the low-temperature water–gas shift (LTWGS) reactor. The two-stage setup is essential because the water–gas shift reaction is moderately exothermic, and according to Le Chatelier's principle, increasing temperature favors the reverse reaction, which limits the extent of conversion. The HTWGS reactor facilitates the initial conversion of CO due to its favorable kinetics but does not achieve full conversion. The LTWGS reactor was then employed for further conversion, allowing the reaction to approach equilibrium [1]. The output stream from the low-temperature water–gas shift reaction was cooled and directed to a flash separator, where residual water was removed from the produced gases before it was sent to the pressure swing adsorption system. To achieve this, the stream was cooled to 38 °C and transported to the flash separator, where the separation of the liquid (water) from the gas stream takes place. The gaseous mixture exiting the flash separator primarily consists of H_2, CO, CO_2, and CH_4. Subsequently, the pressure swing adsorption (PSA) system was employed to separate the hydrogen gas stream from the mixture of other gases. Since Aspen Plus does not include a built-in adsorption system, a combination of a compressor and separator model was used to simulate the separation process achieved in the PSA system. The compressor was employed to increase the pressure to 16 bar, while the separator enhanced the separation of hydrogen from the gaseous stream.

The overall process flowsheet for the pyrolysis and reforming process to produce hydrogen is depicted in Figure 3.

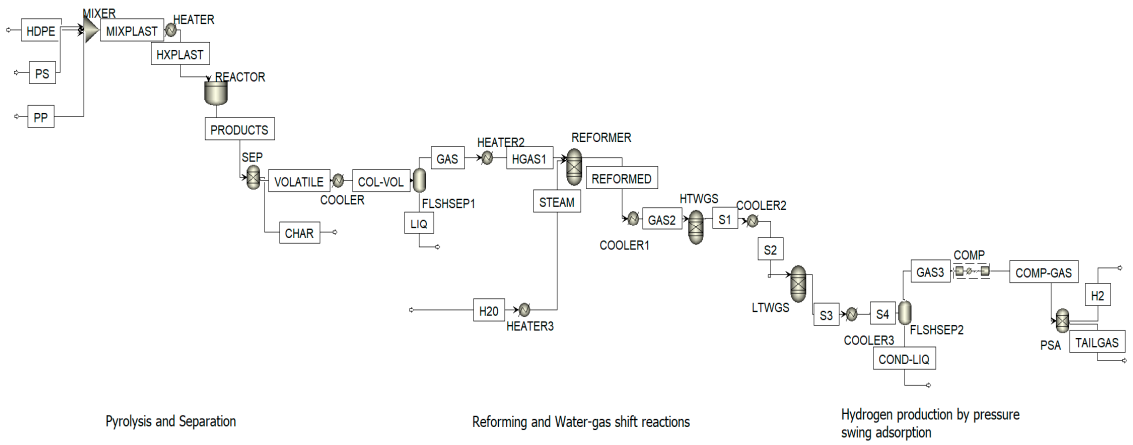

Figure 3. Process flowsheet of pyrolysis and in-line steam reforming simulation on Aspen Plus.

Validation of Model

According to Miranda et al. [64], the stability of polymers, in descending order, is as follows: HDPE > LDPE > PP > PS > PVC. The thermogravimetric analysis (TGA) graph obtained by Miranda et al. [64] illustrating this order is shown in Figure 4.

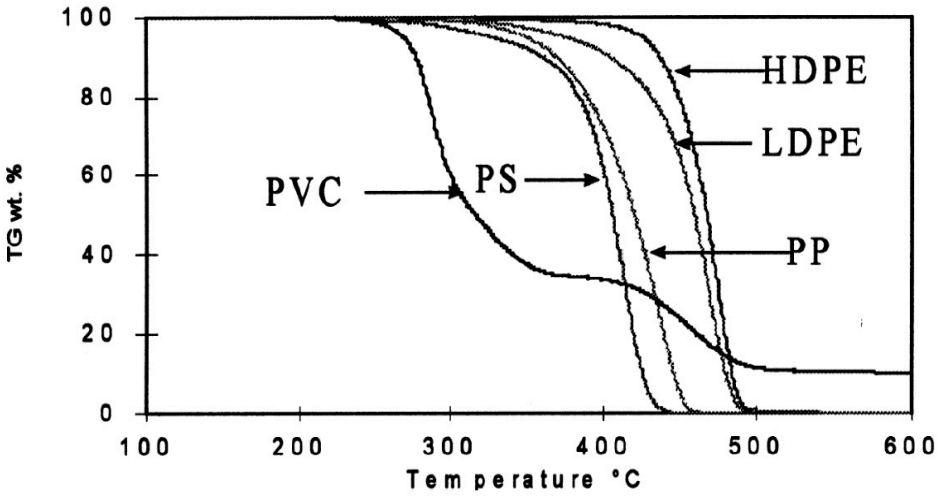

Figure 4. Thermogravimetric curves of various polymers under vacuum at a heating rate of 10 °C/min (fast pyrolysis) [64].

To validate the model obtained from the simulation used in this study, a sensitivity analysis was conducted to evaluate the mass flow of the plastics as the temperature increased. The resulting graph follows the correct order of stability, as shown in Figure 5. The temperature at which each plastic finally decomposes, as depicted in Figure 4, slightly differs from that of Figure 5 because the study conducted by Miranda et al. [64] was based on fast pyrolysis, typically conducted at higher temperatures. In contrast, the data used in this study was based on slow pyrolysis, typically carried out at lower temperatures. This difference in pyrolysis methods accounts for the disparity in decomposition temperatures.

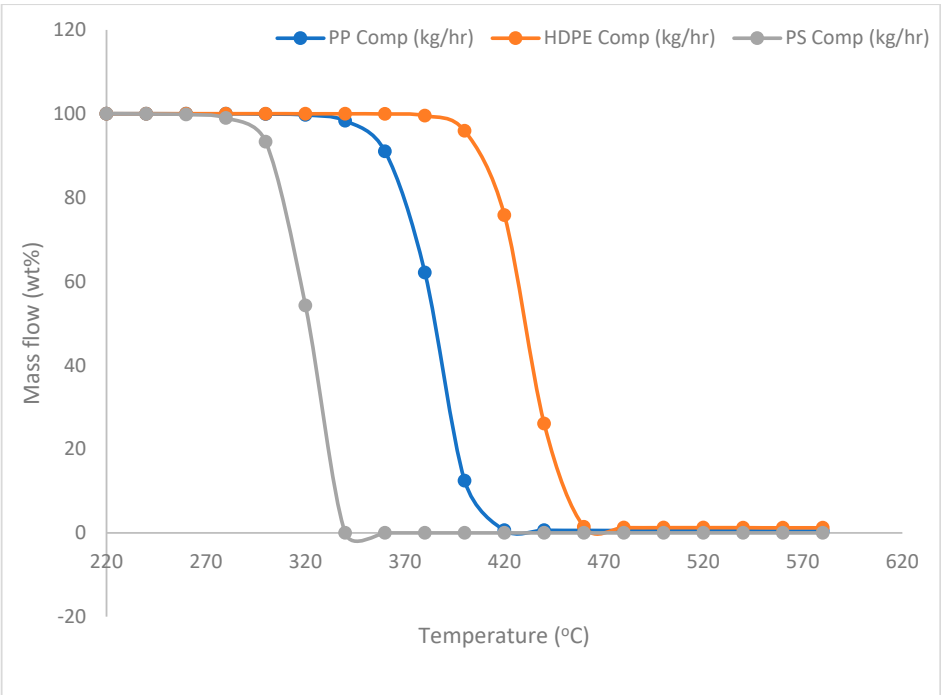

Figure 5. Sensitivity results graph showing plastic decomposition at various temperatures.

3. Results and Discussion

This section provides an in-depth analysis of the evaluation of mixed plastic wastes through pyrolysis and in-line steam reforming. The study examines the impact of key operating parameters on process performance, focusing on the effects of temperature, steam–plastic ratio, and pressure.

3.1. Effect of Reforming Temperature

In the reforming stage of the pyrolysis and in-line reforming process, higher temperatures are typically employed to facilitate the breakdown of hydrocarbon components into syngas, hydrogen, and carbon monoxide. Lopez et al. [65] reported that reforming temperature significantly influences both product yield and gas composition, with elevated temperatures leading to increased hydrogen production. Figure 6 illustrates the effect of temperature on the composition of the gaseous stream (H_2, CO, CO_2, and CH_4) generated during the reforming of the process's gaseous output. It can be observed that the hydrogen yield increased from 17.55 kmol/h at 500 °C to 31.85 kmol/h at 700 °C, beyond which the improvement became negligible.

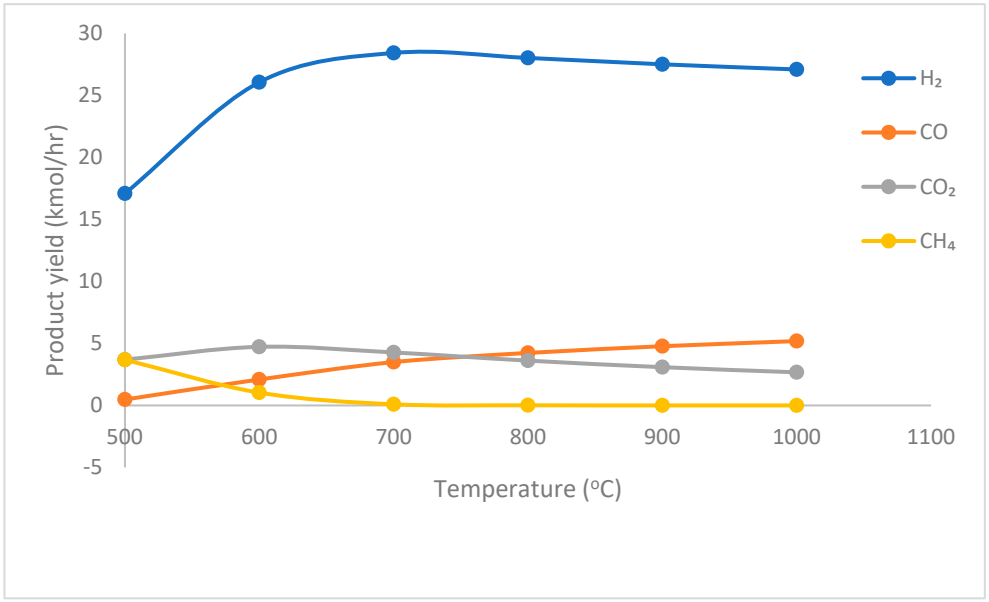

Figure 6. Effect of reforming temperature on gaseous products.

With increasing temperature, CO and H_2 concentrations in the gas phase increase, whereas CH_4 levels decline. The yield of CO_2 initially increases, but as the temperature rises further, it begins to decrease because, at high temperatures, the backward reaction of the exothermic water–gas shift reaction is favored, resulting in the conversion of CO_2 into CO. Generally, the steam reforming reaction enhances the molar ratio of H_2/CO, as evident in Figure 6, where the hydrogen yield surpasses the carbon monoxide yield. At lower temperatures (500 °C), methane concentration is relatively high; however, with increasing temperature, CH_4 concentration declines due to its further conversion to H_2 and CO. This trend aligns with Le Chatelier's principle, which indicates that higher temperatures favor the formation of products in an endothermic reaction, enhancing methane conversion to CO and H_2 in the reformer. Isicheli et al. [52] also demonstrated that increasing the reforming temperature enhances hydrogen yields, rising from 78.1% at 600 °C to 85.7% at 750 °C and attributed this enhancement to the endothermic nature of the reforming reaction, which is favored at elevated temperatures. A similar trend was observed by Yang et al. [66], noting that elevated temperatures create favorable conditions for the thermal

cracking of hydrocarbons. The findings of Wilk et al. [67] in the conversion of mixed plastic wastes confirmed this trend, reporting a decrease in hydrocarbon concentrations from 36% at 640 °C to 21% at 650 °C. This suggests that higher temperatures promote the breakdown of larger carbonaceous molecules into smaller ones, resulting in increased syngas generation [1]. Additionally, the total measured gas compounds increased from 83% at 640 °C to 93% at 760 °C and approaching nearly 100% at 850 °C. This can be attributed to the general principle that higher temperatures accelerate reaction rates, thereby enhancing reforming efficiency. Moreover, they observed a significant rise in H_2 levels, along with increased CO and CO_2 concentrations, aligning with the findings of this study. From Figure 6, the optimum temperature for maximum hydrogen for this study is 700 °C because, beyond 700 °C, the increase is minimal; therefore, for cost-effectiveness, 700 °C is the optimal temperature. Similarly, Lopez et al. [68] reported a maximum hydrogen yield (36%) from HDPE at 700 °C, with 99.4% CH_4 conversion and minimal coke deposition on the Ni commercial catalyst. Erkiaga et al. [29] also conducted HDPE pyrolysis–steam reforming in a spouted bed–fixed bed reactor and reported a high yield of hydrogen (81.5% stoichiometric value) at 700 °C.

3.2. Effect of Steam–Plastic Ratio

Steam plays a crucial role in hydrogen production in the pyrolysis and steam reforming process for waste plastics. Its presence enhances both the reforming process and water–gas shift reactions, resulting in increased gas production, particularly hydrogen [69,70]. Optimizing the steam/plastic ratio (S/P) further improves process efficiency and promotes hydrocarbon cracking [36,69]. The effect of the S/P ratio was investigated at 700 °C and 1 bar. Figure 7 illustrates the influence of the S/P ratio on the mole flow rates of hydrogen, methane, and carbon monoxide.

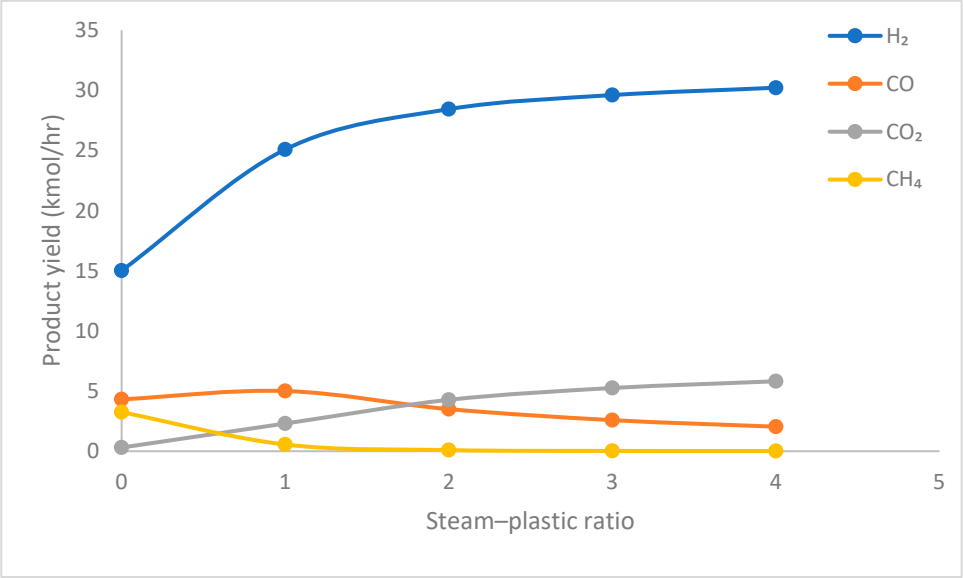

Figure 7. Effect of steam–plastic ratio on hydrogen production.

Various studies have shown that increasing the S/P ratio improves both reforming and water–gas shift reactions for hydrogen production, particularly when the ratio is below 4 [27,31,71,72]. Therefore, the S/P ratio was examined within a range of 0.3 to 4. As the S/P ratio increased from 0.3 to 4, the concentrations of H_2 and CO_2 rose, while those of CO and CH_4 decreased. A similar trend was observed by Pinto et al. [73], where CO, CH_4 and C_nH_m concentrations declined while CO_2 and H_2 levels increased. This indicates that the introduction of steam enhanced hydrogen generation while minimizing tar formation,

facilitating both reforming and water–gas shift reactions. From Figure 7, the hydrogen generation increased from 15.62 kmol/h at S/P = 0 to 31.85 kmol/h at S/P = 2, with a negligible increase after S/P =2. This trend occurs because the presence of additional steam increases the availability of H_2O molecules, driving the reaction toward greater hydrogen production. Furthermore, Barbarias et al. [74] highlighted that the S/P ratio is directly proportional to steam partial pressure, meaning that higher S/P ratios enhance the role of steam partial pressure in the reaction medium, leading to higher conversions. Notably, the highest H_2 yield was achieved at a S/P ratio of 2, after which further increases resulted in only marginal gains. Similarly, other researchers [27,31,33,71] observed that while increasing the S/P ratio initially facilitates the reforming and water–gas shift reactions, its effectiveness diminishes at excessively high ratios.

A high steam–plastic ratio may not be recommended due to its potential drawbacks, including inhibition of catalyst activation, increased costs associated with gas-liquid separation, and the high energy requirements for steam generation. The observed increase in the concentration of H_2 and CO_2 can be attributed to the promotion of water–gas shift reactions facilitated by the presence of steam, converting the produced CO into CO_2 and additional hydrogen. This follows Le Chatelier's principle, which implies that increasing the concentration of a reactant shifts the equilibrium toward more product formation to counteract the change and reduce the added reactants. Lopez et al. [75] reported similar findings when varying the steam–plastic ratio from 0 to 2 at 900 °C in a conical spouted bed reactor. They observed poor performance at an S/P of 0, with hydrogen yield increasing significantly from 28.7 vol% at S/P = 0 to 62 vol% at S/P = 2. Comparable results were reported by Alshareef et al. [47] and Chunfei Wu et al. [76], noting that the increased addition of the steam-to-water gas shift reactor in the presence of a catalyst resulted in higher hydrogen yield.

3.3. Effect of Temperature and Steam–Plastic Ratio

To determine the optimum temperature for the process, the hydrogen yield was evaluated across various temperatures and steam–plastic ratios. Figure 8 illustrates the effect of these operating conditions on hydrogen yield. The temperature range studied was 500 to 1000 °C, while the steam–plastic ratio was varied from 0.3 to 4.

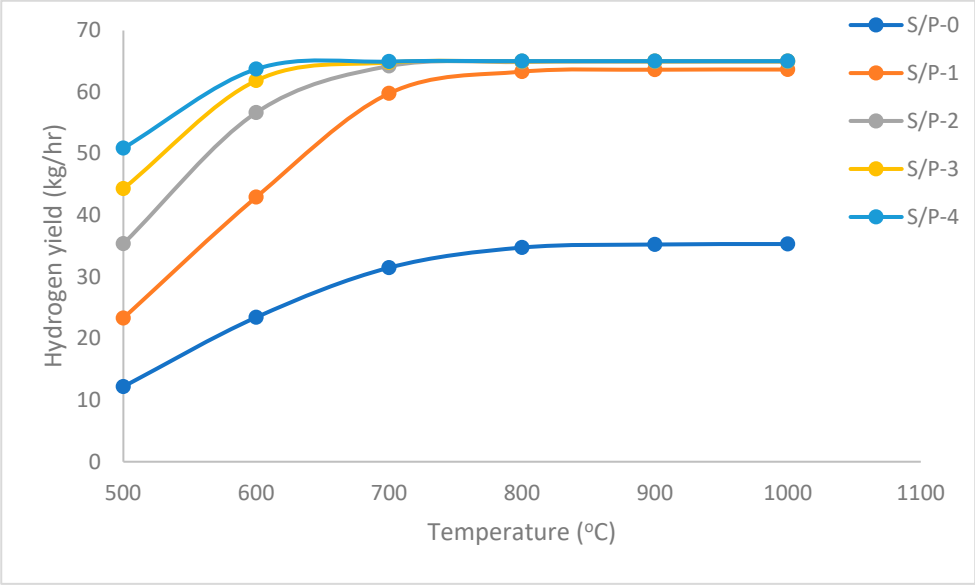

Figure 8. Effect of Steam–plastic ratio and temperature on hydrogen production.

As previously noted, increasing the temperature at various steam–plastic ratios resulted in higher hydrogen yields due to enhanced reforming reaction efficiency. At a low S/P ratio (S/P = 0), hydrogen yield increased with rising temperature. However, as the S/P ratio increased, the hydrogen yield showed a more pronounced rise with temperature. Notably, at S/P ratios above 2, hydrogen production continued to increase between 500 °C and 700 °C, but the differences became negligible beyond this range. Thus, the optimal temperature for reforming was determined to be 700 °C, with an optimal S/P ratio of 2. Higher values would only lead to increased energy demand for steam generation without significantly improving the process, thereby escalating energy costs and expenses related to gas-liquid separation.

3.4. Effect of Pressure and Steam–Plastic Ratio

The effect of varying pressures on the production of hydrogen was also examined. Figure 9 shows the interaction between steam–plastic ratio and pressure in hydrogen production. While increasing the S/P ratio enhances hydrogen production due to the availability of sufficient steam to drive both the steam reforming and water–gas shift reactions, it was observed that increasing the pressure above 1 bar diminishes the positive effect of a higher S/P ratio. This can be attributed to Le Chatelier's principle, which states that at elevated pressures, the equilibrium shifts towards the side with lower moles of gas. In the case of the reforming reactions (as shown in Equations (3)–(9)), it suppresses hydrocarbon cracking and reduces the efficiency of hydrogen generation. Elevated pressures also promote the retention of unreacted hydrocarbons, such as methane, leading to less effective conversion in the reformer. This is illustrated in Figure 9, which shows an increase in methane concentration and a corresponding decrease in hydrogen and carbon monoxide concentrations at higher pressures.

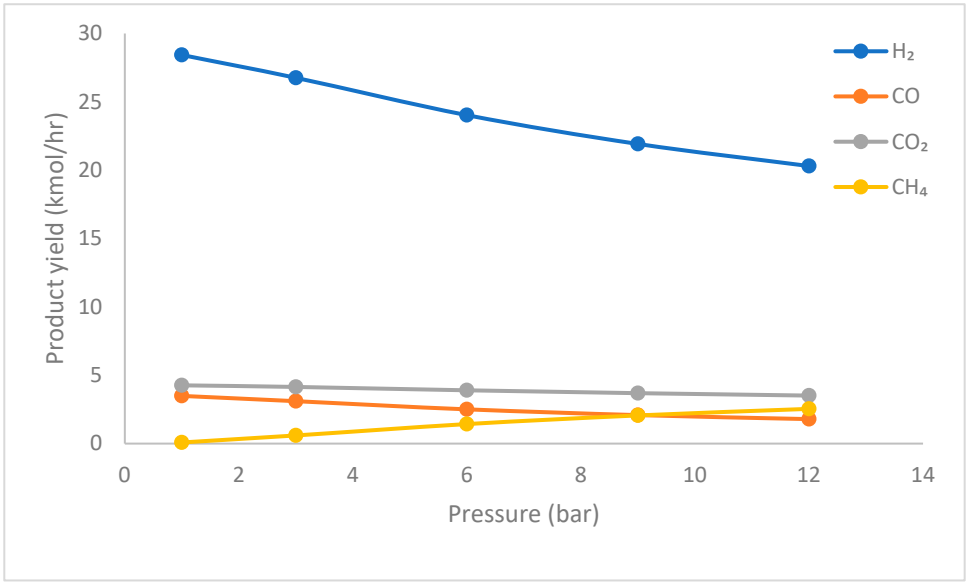

Figure 9. Effect of pressure on gaseous composition.

Figure 10 indicates that hydrogen yield decreases with increasing pressure. However, at all pressure levels, hydrogen yield improves as the steam–plastic ratio increases. This suggests that while elevated pressures can limit hydrogen production, optimizing the steam–plastic ratio can help mitigate this effect by ensuring adequate steam availability for the reforming reactions. Based on these findings, the optimal pressure for hydrogen production is 1 bar, as higher pressures result in reduced hydrogen yield.

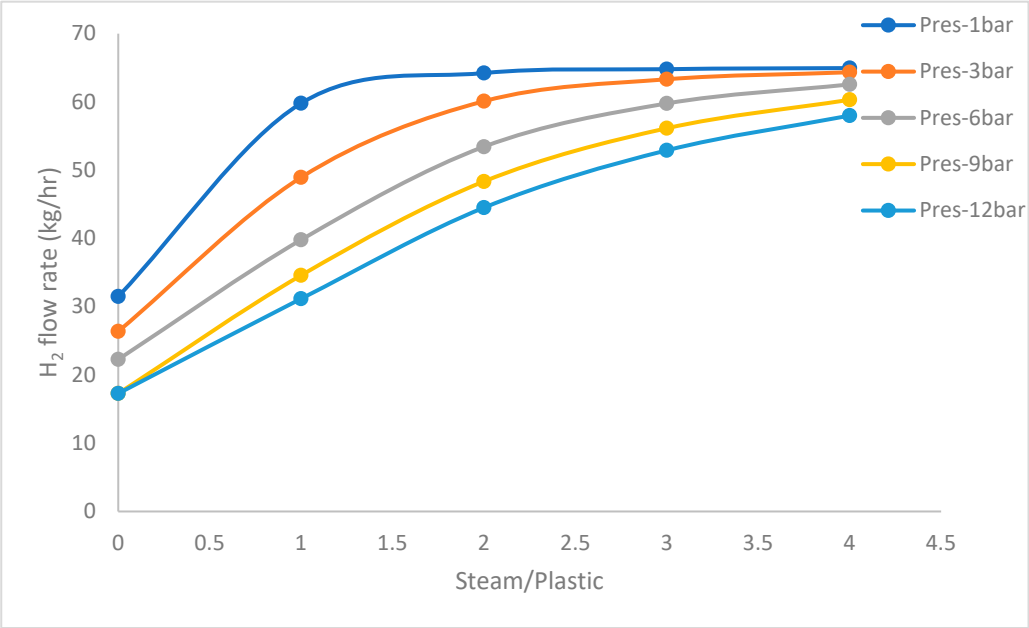

Figure 10. Effect of pressure and steam–plastic ratio on hydrogen production.

3.5. Hydrogen Yield Optimization

The optimized hydrogen yield in this study reached 31.85 kmol/h (64.21 kg/h) at 700 °C and a steam-to-plastic (S/P) ratio of 2. This result is notable when compared to previous studies. For instance, Li et al. [77] reported hydrogen yields ranging from 36.84 to 39.08 wt% at 900 °C from single polyolefin plastic types using a two-stage pyrolysis and catalytic steam reforming process. Additionally, Barbarias et al. [78] achieved 29.1 wt% hydrogen production through a similar two-stage process for polystyrene, emphasizing the effectiveness of catalytic steam reforming in hydrogen generation from waste plastics. These studies utilized higher reforming temperatures and different feedstock compositions. The current study's approach not only achieves a comparable yield but does so at a relatively moderate temperature, thereby enhancing process efficiency.

4. Conclusions

A simulation model was developed to analyze the impact of operating parameters on the pyrolysis and in-line steam reforming process for plastic wastes. This study investigated the effects of temperature, steam–plastic ratio, and pressure on gas production, particularly hydrogen. The results showed that increasing the temperature from 500 °C to 700 °C significantly enhanced hydrogen yield, rising from 17.55 kmol/h to 31.85 kmol/h. The maximum hydrogen yield was achieved at 700 °C and 1 bar. The steam-to-plastic ratio, also a critical parameter affecting the pyrolysis-reforming reactions, played a significant role in enhancing the reforming and water–gas shift reaction. An S/P ratio of 2 was identified as optimal for achieving a favorable H_2/CO ratio, promoting hydrogen production. Additionally, higher pressures were observed to decrease hydrogen yield. In conclusion, optimizing temperature, steam–plastic ratio, and pressure (i.e., higher temperature, greater steam–plastic ratios, and lower pressures) can significantly enhance hydrogen yield in the pyrolysis and in-line steam reforming of mixed plastic waste.

Author Contributions: Conceptualization, F.J.M. and H.R.N.; methodology, F.J.M.; software, F.J.M.; validation, F.J.M.; formal analysis, F.J.M.; investigation, F.J.M. and H.R.N.; resources, F.J.M. and H.R.N.; data curation, F.J.M.; writing—original draft preparation, F.J.M.; writing—review and editing,

F.J.M. and H.R.N.; visualization, F.J.M.; supervision, H.R.N., K.K and L.K.; project administration, H.R.N., K.K. and L.K.; All authors have read and agreed to the published version of the manuscript.

Funding: This research received no external funding.

Data Availability Statement: All relevant data for this study are provided in the paper.

Acknowledgments: The author extends sincere gratitude to the Commonwealth Scholarship Commission and the Foreign, Commonwealth, and Development office in the UK for their invaluable support, which made the research presented in this article possible. Gratitude is also extended to the University of Central Lancashire for their collaboration in sponsoring this research.

Conflicts of Interest: The authors declare no conflicts of interest.

References

1. Lahafdoozian, M.; Khoshkroudmansouri, H.; Zein, S.H.; Jalil, A.A. Hydrogen production from plastic waste: A comprehensive simulation and machine learning study. *Int. J. Hydrogen Energy* **2024**, *59*, 465–479. [CrossRef]
2. Jakovac, P. The Influence of Energy Trends on the Global Economy. *In Book of Abstracts*. 2022, pp. 299–308. Available online: https://eman-conference.org/energy-trends-on-global-economy/ (accessed on 30 September 2024).
3. Kamara-Esteban, O.; Pijoan, A.; Alonso-Vicario, A.; Borges, C.E. On-demand energy monitoring and response architecture in a ubiquitous world. *Pers. Ubiquitous Comput.* **2017**, *21*, 537–551. [CrossRef]
4. Soroush, M.; Shahbakhti, M. Special issue on 'Optimal design and operation of energy systems. *Optim. Control. Appl. Methods* **2023**, *44*, 351–354. [CrossRef]
5. Dawood, F.; Anda, M.; Shafiullah, G.M. Hydrogen production for energy: An overview. *Int. J. Hydrogen Energy* **2020**, *45*, 3847–3869. [CrossRef]
6. Rohland, B.; Nitsch, J.; Wendt, H. Hydrogen and fuel cells—The clean energy system. *J. Power Sources* **1992**, *37*, 271–277. [CrossRef]
7. Hosseini, S.E.; Wahid, M.A. Hydrogen production from renewable and sustainable energy resources: Promising green energy carrier for clean development. *Renew. Sustain. Energy Rev.* **2016**, *57*, 850–866. [CrossRef]
8. Mohr, T.; Aliyu, H.; Biebinger, L.; Gödert, R.; Hornberger, A.; Cowan, D.; de Maayer, P.; Neumann, A. Effects of different operating parameters on hydrogen production by Parageobacillus thermoglucosidasius DSM 6285. *AMB Express* **2019**, *9*, 207. [CrossRef]
9. Singla, M.K.; Nijhawan, P.; Oberoi, A.S. Hydrogen fuel and fuel cell technology for cleaner future: A review. *Environ. Sci. Pollut. Res.* **2021**, *28*, 15607–15626. [CrossRef]
10. Shadidi, B.; Najafi, G.; Yusaf, T. A Review of Hydrogen as a Fuel in Internal Combustion Engines. *Energies* **2021**, *14*, 6209. [CrossRef]
11. Gholami, S.; Rostaminikoo, E.; Khajenoori, L.; Nasriani, H.R. Density determination of CO_2-Rich fluids within CCUS processes. In *Measurement: Sensors*; Elsevier Ltd.: Amsterdam, The Netherlands, 2025. [CrossRef]
12. Nasriani, H.R.; Jamiolahmady, M. Optimising Flowback Strategies in Unconventional Reservoirs: The Critical Role of Capillary Forces and Fluid Dynamics. *Energies* **2024**, *17*, 5822. [CrossRef]
13. Gandomkar, A.; Torabi, F.; Nasriani, H.R.; Enick, R.M. Decreasing Asphaltene Precipitation and Deposition during Immiscible Gas Injection Via the Introduction of a CO_2-Soluble Asphaltene Inhibitor. *SPE J.* **2023**, *28*, 2316–2328. [CrossRef]
14. Nasriani, H.R.; Kalantari Asl, A. Choke Performance in High-rate Gas Condensate Wells Under Subcritical Flow Condition. *Energy Sources Part A Recovery Util. Environ. Eff.* **2014**, *37*, 192–199. [CrossRef]
15. Nasriani, H.R.; Jamiolahmady, M. Flowback cleanup mechanisms of post-hydraulic fracturing in unconventional natural gas reservoirs. *J. Nat. Gas Sci. Eng.* **2019**, *66*, 316–342. [CrossRef]
16. Nasriani, H.R.; Jamiolahmady, M.; Saif, T.; Sánchez, J. A systematic investigation into the flowback cleanup of hydraulic-fractured wells in unconventional gas plays. *Int. J. Coal Geol.* **2018**, *193*, 46–60. [CrossRef]
17. Alvarez, J.; Kumagai, S.; Wu, C.; Yoshioka, T.; Bilbao, J.; Olazar, M.; Williams, P.T. Hydrogen production from biomass and plastic mixtures by pyrolysis-gasification. *Int. J. Hydrogen Energy* **2014**, *39*, 10883–10891. [CrossRef]
18. Smith, L. Plastic Waste. Mar. 2024, House of Commons Library, Research Briefing. Available online: https://researchbriefings.files.parliament.uk/documents/CBP-8515/CBP-8515.pdf (accessed on 10 September 2024).
19. Medaiyese, F.J.; Nasriani, H.R.; Khajenoori, L.; Khan, K.; Badiei, A. From Waste to Energy: Enhancing Fuel and Hydrogen Production through Pyrolysis and In-Line Reforming of Plastic Wastes. *Sustainability* **2024**, *16*, 4973. [CrossRef]
20. Barbarias, I.; Lopez, G.; Artetxe, M.; Arregi, A.; Bilbao, J.; Olazar, M. Valorisation of different waste plastics by pyrolysis and in-line catalytic steam reforming for hydrogen production. *Energy Convers. Manag.* **2018**, *156*, 575–584. [CrossRef]
21. Cortazar, M.; Gao, N.; Quan, C.; Suarez, M.A.; Lopez, G.; Orozco, S.; Santamaria, L.; Amutio, M.; Olazar, M. Analysis of hydrogen production potential from waste plastics by pyrolysis and in line oxidative steam reforming. *Fuel Process. Technol.* **2022**, *225*, 107044. [CrossRef]

22. Koike, M.; Li, D.; Watanabe, H.; Nakagawa, Y.; Tomishige, K. Comparative study on steam reforming of model aromatic compounds of biomass tar over Ni and Ni–Fe alloy nanoparticles. *Appl. Catal. A Gen.* **2015**, *506*, 151–162. [CrossRef]
23. Devi, L.; Ptasinski, K.J.; Janssen, F.J. A review of the primary measures for tar elimination in biomass gasification processes. *Biomass Bioenergy* **2003**, *24*, 125–140. [CrossRef]
24. Shah, H.H.; Amin, M.; Iqbal, A.; Nadeem, I.; Kalin, M.; Soomar, A.M.; Galal, A.M. A review on gasification and pyrolysis of waste plastics. *Front. Chem.* **2023**, *10*, 960894. [CrossRef] [PubMed]
25. Guan, G.; Kaewpanha, M.; Hao, X.; Abudula, A. Catalytic steam reforming of biomass tar: Prospects and challenges. *Renew. Sustain. Energy Rev.* **2016**, *58*, 450–461. [CrossRef]
26. Anis, S.; Zainal, Z.A. Tar reduction in biomass producer gas via mechanical, catalytic and thermal methods: A review. *Renew. Sustain. Energy Rev.* **2011**, *15*, 2355–2377. [CrossRef]
27. Tsuji, T.; Hatayama, A. Gasification of waste plastics by steam reforming in a fluidized bed. *J. Mater. Cycles Waste Manag.* **2009**, *11*, 144–147. [CrossRef]
28. Park, Y.; Namioka, T.; Sakamoto, S.; Min, T.; Roh, S.; Yoshikawa, K. Optimum operating conditions for a two-stage gasification process fueled by polypropylene by means of continuous reactor over ruthenium catalyst. *Fuel Process. Technol.* **2010**, *91*, 951–957. [CrossRef]
29. Erkiaga, A.; Lopez, G.; Barbarias, I.; Artetxe, M.; Amutio, M.; Bilbao, J.; Olazar, M. HDPE pyrolysis-steam reforming in a tandem spouted bed-fixed bed reactor for H2 production. *J. Anal. Appl. Pyrolysis* **2015**, *116*, 34–41. [CrossRef]
30. Namioka, T.; Saito, A.; Inoue, Y.; Park, Y.; Min, T.J.; Roh, S.A.; Yoshikawa, K. Hydrogen-rich gas production from waste plastics by pyrolysis and low-temperature steam reforming over a ruthenium catalyst. *Appl. Energy* **2011**, *88*, 2019–2026. [CrossRef]
31. Barbarias, I.; Lopez, G.; Alvarez, J.; Artetxe, M.; Arregi, A.; Bilbao, J.; Olazar, M. A sequential process for hydrogen production based on continuous HDPE fast pyrolysis and in-line steam reforming. *Chem. Eng. J.* **2016**, *296*, 191–198. [CrossRef]
32. Arregi, A.; Lopez, G.; Amutio, M.; Barbarias, I.; Bilbao, J.; Olazar, M. Hydrogen production from biomass by continuous fast pyrolysis and in-line steam reforming. *RSC Adv.* **2016**, *6*, 25975–25985. [CrossRef]
33. Bashir, M.A.; Tuo, J.; Weidman, J.; Soong, Y.; Gray, M.L.; Shi, F.; Wang, P. Plastic waste gasification for low-carbon hydrogen production: A comprehensive review. *Energy Adv.* **2025**. [CrossRef]
34. Jeong, Y.-S.; Park, K.-B.; Kim, J.-S. Hydrogen production from steam gasification of polyethylene using a two-stage gasifier and active carbon. *Appl. Energy* **2020**, *262*, 114495. [CrossRef]
35. Lopez, G.; Artetxe, M.; Amutio, M.; Alvarez, J.; Bilbao, J.; Olazar, M. Recent advances in the gasification of waste plastics. A critical overview. *Renew. Sustain. Energy Rev.* **2018**, *82*, 576–596. [CrossRef]
36. Erkiaga, A.; Lopez, G.; Amutio, M.; Bilbao, J.; Olazar, M. Syngas from steam gasification of polyethylene in a conical spouted bed reactor. *Fuel* **2013**, *109*, 461–469. [CrossRef]
37. Chai, Y.; Gao, N.; Wang, M.; Wu, C. H2 production from co-pyrolysis/gasification of waste plastics and biomass under novel catalyst Ni-CaO-C. *Chem. Eng. J.* **2020**, *382*, 122947. [CrossRef]
38. Williams, P.T. *Hydrogen and Carbon Nanotubes from Pyrolysis-Catalysis of Waste Plastics: A Review*; Springer Science and Business Media B.V.: Berlin/Heidelberg, Germany, 2021. [CrossRef]
39. Arregi, A.; Seifali Abbas-Abadi, M.; Lopez, G.; Santamaria, L.; Artetxe, M.; Bilbao, J.; Olazar, M. CeO_2 and La_2O_3 Promoters in the Steam Reforming of Polyolefinic Waste Plastic Pyrolysis Volatiles on Ni-Based Catalysts. *ACS Sustain. Chem. Eng.* **2020**, *8*, 17307–17321. [CrossRef]
40. Arregi, A.; Lopez, G.; Amutio, M.; Artetxe, M.; Barbarias, I.; Bilbao, J.; Olazar, M. Role of operating conditions in the catalyst deactivation in the in-line steam reforming of volatiles from biomass fast pyrolysis. *Fuel* **2018**, *216*, 233–244. [CrossRef]
41. Bobek-Nagy, J.; Gao, N.; Quan, C.; Miskolczi, N.; Rippel-Pethő, D.; Kovács, K. Catalytic co-pyrolysis of packaging plastic and wood waste to achieve H_2 rich syngas. *Int. J. Energy Res.* **2020**, *44*, 10832–10845. [CrossRef]
42. Pandey, B.; Prajapati, Y.K.; Sheth, P.N. Recent progress in thermochemical techniques to produce hydrogen gas from biomass: A state of the art review. *Int. J. Hydrogen Energy* **2019**, *44*, 25384–25415. [CrossRef]
43. Arregi, A.; Amutio, M.; Lopez, G.; Bilbao, J.; Olazar, M. Evaluation of thermochemical routes for hydrogen production from biomass: A review. *Energy Convers. Manag.* **2018**, *165*, 696–719. [CrossRef]
44. Joonaki, E.; Rostaminikoo, E.; Ghanaatian, S.; Nasriani, H.R. Thermodynamic properties of hydrogen containing systems and calculation of gas critical flow factor. In *Measurement: Sensors*; Elsevier Ltd.: Amsterdam, The Netherlands, 2025. [CrossRef]
45. Rostaminikoo, E.; Ghanaatian, S.; Joonaki, E.; Nasriani, H.R.; Whitton, J. Advanced thermodynamics of hydrogen and natural gas blends for gas transmission and distribution networks. In *Measurement: Sensors*; Elsevier Ltd.: Amsterdam, The Netherlands, 2025. [CrossRef]
46. Joonaki, E.; Rostaminikoo, E.; Ghanaatian, S.; Nasriani, H. Thermodynamics of Hydrogen; Analysing and Refining of Critical Flow Factor Through Comprehensive Uncertainty Assessment and Experimental Data Integration. In Proceedings of the Abu Dhabi International Petroleum Exhibition and Conference, Abu Dhabi, United Arab Emirates, 4–7 November 2024. [CrossRef]

47. Alshareef, R.; Nahil, M.A.; Williams, P.T. Hydrogen Production by Three-Stage (i) Pyrolysis, (ii) Catalytic Steam Reforming, and (iii) Water Gas Shift Processing of Waste Plastic. *Energy Fuels* **2023**, *37*, 3894–3907. [CrossRef]
48. Han, D.; Shin, S.; Jung, H.; Cho, W.; Baek, Y. Hydrogen Production by Steam Reforming of Pyrolysis Oil from Waste Plastic over 3 wt.% Ni/Ce-Zr-Mg/Al2O3 Catalyst. *Energies* **2023**, *16*, 2656. [CrossRef]
49. Pawelczyk, E.; Wysocka, I.; Gębicki, J. Pyrolysis Combined with the Dry Reforming of Waste Plastics as a Potential Method for Resource Recovery—A Review of Process Parameters and Catalysts. *Catalysts* **2022**, *12*, 362. [CrossRef]
50. Soleimani, S.; Methane, M.L.T.-R.O.; Conditions, O. Reactor Technology and Efficiency Evaluation—A Review. *Energies* **2022**, *15*, 7159. [CrossRef]
51. Barbarias, I.; Artetxe, M.; Lopez, G.; Arregi, A.; Bilbao, J.; Olazar, M. Influence of the conditions for reforming HDPE pyrolysis volatiles on the catalyst deactivation by coke. *Fuel Process. Technol.* **2018**, *171*, 100–109. [CrossRef]
52. Isicheli, P.; Oji, A.; Okwonna, O.; Muwarure, P.; Ibrahim, A.D.; Erazele, A. Analysing the effects of process parameters on HDPE pyrolysis and in-line reforming. *Glob. J. Eng. Technol. Adv.* **2023**, *17*, 139–149. [CrossRef]
53. Sachin, S.; Kumar, K. Conversion of Waste High-Density Polyethylene into Liquid Fuels, National Institute of Technology Rourkela. *Chem. Eng.* 2014. Available online: https://core.ac.uk/download/pdf/53189114.pdf (accessed on 8 October 2024).
54. Sarker, M. Converting waste plastic to hydrocarbon fuel materials. *Energy Eng. J. Assoc. Energy Eng.* **2011**, *108*, 35–43. [CrossRef]
55. Jaafar, Y.; Abdelouahed, L.; El Hage, R.; El Samrani, A.; Taouk, B. Pyrolysis of common plastics and their mixtures to produce valuable petroleum-like products. *Polym. Degrad. Stab.* **2022**, *195*, 109770. [CrossRef]
56. Gebre, S.H.; Sendeku, M.G.; Bahri, M. *Recent Trends in the Pyrolysis of Non-Degradable Waste Plastics*; John Wiley and Sons Inc.: Hoboken, NJ, USA, 2021. [CrossRef]
57. Levine, S.E.; Broadbelt, L.J. Detailed mechanistic modeling of high-density polyethylene pyrolysis: Low molecular weight product evolution. *Polym. Degrad. Stab.* **2009**, *94*, 810–822. [CrossRef]
58. Kruse, T.M.; Wong, H.-W.; Broadbelt, L.J. Mechanistic modeling of polymer pyrolysis: Polypropylene. *Macromolecules* **2003**, *36*, 9594–9607. [CrossRef]
59. Kruse, T.M.; Woo, O.S.; Wong, H.-W.; Khan, S.S.; Broadbelt, L.J. Mechanistic Modeling of Polymer Degradation: A Comprehensive Study of Polystyrene. *Macromolecules* **2002**, *35*, 7830–7844. [CrossRef]
60. Aspen Technology. *Pyrolysis of High-Density Polyethylene*; Aspen Technology: Bedford, MA, USA, 2022.
61. Aspen Technology. *Polypropylene Pyrolysis*; Aspen Technology: Bedford, MA, USA, 2022.
62. Aspen Technology. *Polystyrene Pyrolysis*; Aspen Technology: Bedford, MA, USA, 2022.
63. Phan, T.S.; Minh, D.P.; Espitalier, F.; Nikou, A.; Grouset, D. Hydrogen production from biogas: Process optimization using ASPEN Plus®. *Int. J. Hydrogen Energy* **2022**, *47*, 42027–42039. [CrossRef]
64. Miranda, R.; Yang, J.; Roy, C.; Vasile, C. Vacuum pyrolysis of commingled plastics containing PVC I. Kinetic study. *Polym. Degrad. Stab.* **2001**, *72*, 469–491. [CrossRef]
65. López, A.; de Marco, I.; Caballero, B.M.; Laresgoiti, M.F.; Adrados, A. Influence of time and temperature on pyrolysis of plastic wastes in a semi-batch reactor. *Chem. Eng. J.* **2011**, *173*, 62–71. [CrossRef]
66. Yang, Y.; Zhu, J.; Zhu, G.; Yang, L.; Zhu, Y. The effect of high temperature on syngas production by immediate pyrolysis of wet sewage sludge with sawdust. *J. Therm. Anal. Calorim.* **2018**, *132*, 1783–1794. [CrossRef]
67. Wilk, V.; Hofbauer, H. Conversion of mixed plastic wastes in a dual fluidized bed steam gasifier. *Fuel* **2013**, *107*, 787–799. [CrossRef]
68. Lopez, G.; Erkiaga, A.; Artetxe, M.; Amutio, M.; Bilbao, J.; Olazar, M. Hydrogen Production by High Density Polyethylene Steam Gasification and In-Line Volatile Reforming. *Ind. Eng. Chem. Res.* **2015**, *54*, 9536–9544. [CrossRef]
69. Li, Y.; Nahil, M.A.; Williams, P.T. Pyrolysis-catalytic steam reforming of waste plastics for enhanced hydrogen/syngas yield using sacrificial tire pyrolysis char catalyst. *Chem. Eng. J.* **2023**, *467*, 143427. [CrossRef]
70. Turn, S. An experimental investigation of hydrogen production from biomass gasification. *Int. J. Hydrogen Energy* **1998**, *23*, 641–648. [CrossRef]
71. Li, J.; Liao, S.; Dan, W.; Jia, K.; Zhou, X. Experimental study on catalytic steam gasification of municipal solid waste for bioenergy production in a combined fixed bed reactor. *Biomass Bioenergy* **2012**, *46*, 174–180. [CrossRef]
72. Wang, Y.; Kinoshita, C.M. Experimental analysis of biomass gasification with steam and oxygen. *Solar Energy* **1992**, *49*, 153–158. [CrossRef]
73. Pinto, F.; Franco, C.; André, R.N.; Miranda, M.; Gulyurtlu, I.; Cabrita, I. Co-gasification study of biomass mixed with plastic wastes. *Fuel* **2002**, *81*, 291–297. [CrossRef]
74. Barbarias, I.; Arregi, A.; Artetxe, M.; Santamaria, L.; Lopez, G.; Cortazar, M.; Amutio, M.; Bilbao, J.; Olazar, M. Waste Plastics Valorization by Fast Pyrolysis and in Line Catalytic Steam Reforming for Hydrogen Production. In *Recent Advances in Pyrolysis*; IntechOpen: London, UK, 2020. [CrossRef]

75. Lopez, G.; Erkiaga, A.; Amutio, M.; Alvarez, J.; Barbarias, I.; Bilbao, J.; Olazar, M. Steam Gasification of Waste Plastics in a Conical Spouted Bed Reactor. In Proceedings of the 14th International Conference on Fluidization—From Fundamentals to Products, Noordwijkerhout, The Netherlands, 26–31 May 2013. ECI Symposium Series.
76. Wu, C.; Nahil, M.A.; Miskolczi, N.; Huang, J.; Williams, P.T. Processing Real-World Waste Plastics by Pyrolysis-Reforming for Hydrogen and High-Value Carbon Nanotubes. *Environ. Sci. Technol.* **2014**, *48*, 819–826. [CrossRef] [PubMed]
77. Li, Y.; Nahil, M.A.; Williams, P.T. Hydrogen/Syngas Production from Different Types of Waste Plastics Using a Sacrificial Tire Char Catalyst via Pyrolysis–Catalytic Steam Reforming. *Energy Fuels* **2023**, *37*, 6661–6673. [CrossRef]
78. Barbarias, I.; Lopez, G.; Artetxe, M.; Arregi, A.; Santamaria, L.; Bilbao, J.; Olazar, M. Pyrolysis and in-line catalytic steam reforming of polystyrene through a two-step reaction system. *J. Anal. Appl. Pyrolysis* **2016**, *122*, 502–510. [CrossRef]